INFLUENCE OF BREAK UP AND COALESCENCE MODELS IN A BUBBLY FLOW

Marcela K. Silva, Renato P. Dionísio, Marcos A. d'Ávila, Milton Mori
School of Chemical Engineering, University of Campinas, UNICAMP, Campinas-SP, Brazil

Abstract

Three-dimensional gas-liquid simulations in a cylindrical bubble reactor with an external loop were performed. The effects of average bubble size, bubble size distribution and gas inlet plate geometry were evaluated. The population balance models of Luo and Svendsen [6] and Prince and Blanch [9] were used in order to simulate the breakup and coalescence effects, respectively. The drag force was modeled using the Ishii-Zuber model, which takes into account bubble deformation effects. The k-epsilon turbulence model was applied only for the continuous phase and the dispersed one was considered laminar. Lift, Magnus and added mass forces were neglected. Simulations at different superficial gas velocities were performed using two different inlets: a uniform and a perforated plate entrance. Breakup and coalescence effects were studied only for the uniform gas inlet geometry and the particle size distribution was obtained using a probability density function. Results show that the approach used in this work provided physically consistent results with transient effects in the column. Good agreement of the time-averaged gas holdup with experimental data on gas holdup available in the literature was obtained. It was found that the simulation approach used in this work was able to capture the complex transient fluid dynamics in bubbly flows.

Introduction

Bubble column reactors are found in many applications in chemical reaction engineering. They are encountered, among others, in biochemical process and slurry reactors for Fischer-Tropsch synthesis [7]. One of the main characteristics that determine the proper performance of a bubble reactor is the fluid dynamics inside the column, which is very complex since it is highly turbulent multiphase flow with chaotic dynamics [2].

However, the use of the adequate available tools can be very important in developing scale-up strategies and for the understanding of its flow behavior. Due to the arising of high speed computers and the advancement of numerical techniques, numerical studies of bubbly flows have increased. These numerical techniques are now capable to perform three-dimensional simulations of multiphase flows in complex geometries.

Gas-liquid fluidization systems operate by the injection of the gas phase in the bottom of a column filled with liquid. This operation depends on several factors such as fluid physical properties, column dimensions and inlet gas velocity. There are basically two kinds of flow regimes: the homogeneous and the heterogeneous. The homogeneous flow regime is characterized by low superficial gas velocity, and the bubbles are nearly uniform in size and shape, where bubble breakup and coalescence are considered to be insignificant. On the other hand, in the heterogeneous flow regime, where the superficial gas velocity is high, it is observed higher turbulence, inducing bubble break up and coalescence; in this case, models that are able to capture these phenomena are necessary.

Computational fluid dynamics (CFD) studies have been carried out aiming the scale-up of slurry reactors [11], the modeling of the churn-turbulent flow regime, the presence of catalyst through three-phase flow simulations [8], the break up and coalescence of bubbles [3], the mass transfer [13] and chemical reactions [11], among others. However, there are important issues that have been investigated and a consensus has not been achieved. Studies can be found in evaluation of columns of different sizes in order to test and obtain scale-up correlations based on CFD simulations [4], as well as the effect of gas sparger [1], drag modeling and internals [10].

In the present work, it is showed a three-dimensional gas-liquid simulation in a cylindrical bubble reactor with an external loop using the Eulerian-Eulerian approach. The commercial CFD package CFX 11 from ANSYS, which uses the finite volume method to solve the discretized system of equations that represents the flow, was used. The aim of this study is to present the effects of important parameters in CFD simulations, such as bubble size and geometrical modeling of gas sparger.

Results have shown that the approach used in this work provided physically consistent results, showing the transient effects in the column. Good agreement of time-averaged gas holdup with experimental data of gas holdup available in the literature was obtained. It was found that the simulation approach used in this work was able to capture the transient fluid dynamics.

Mathematical Modeling

The equations used to describe bubbly flows in the present work are the mass and momentum conservation equations, which consider the interaction between the phases using an Eulerian-Eulerian approach, given respectively by

$$\frac{\partial}{\partial t}(\varphi_\alpha \rho_\alpha) + \nabla \bullet \left(\varphi_\alpha \rho_\alpha \vec{U}_\alpha\right) = 0 \qquad (1)$$

$$\frac{\partial}{\partial t}\left(\varphi_\alpha \rho_\alpha \vec{U}_\alpha\right) + \nabla \bullet \left(\varphi_\alpha (\rho_\alpha \vec{U}_\alpha \vec{U}_\alpha)\right) = \varphi_\alpha \nabla P_\alpha + \nabla \bullet \left(\varphi_\alpha \mu_\alpha \left(\nabla \overrightarrow{U_\alpha} + \left(\nabla \overrightarrow{U_\alpha}\right)^T\right)\right) + M_\alpha + \rho_\alpha \vec{g}\,. \qquad (2)$$

Here, ρ is the density, φ is the volume fraction, $\vec{U}$ is the velocity vector, μ is the viscosity and M_α are the interphase forces, which are the sums of all forces:

$$M_\alpha = \sum_{\beta \neq \alpha} M_{\alpha\beta} = M_{\alpha\beta}^D + M_{\alpha\beta}^L + M_{\alpha\beta}^{LUB} + M_{\alpha\beta}^{VM} + M_{\alpha\beta}^{TD} + ..., \qquad (3)$$

where α and β indicate continuous and dispersed phases, $M_{\alpha\beta}^D$ is the drag force, $M_{\alpha\beta}^L$ is the lift force, $M_{\alpha\beta}^{LUB}$ is the wall lubrification force, $M_{\alpha\beta}^{VM}$ is the virtual mass force and $M_{\alpha\beta}^{TD}$ is the turbulence dispersion force. In this study only the drag force, which is the main interphase force affecting the bubble column flow, was considered. The mathematical term is given by

$$M_{\alpha\beta}^D = \frac{C_D}{8} A_{gl} \rho_l \left(\overrightarrow{U_l} - \overrightarrow{U_g}\right)\left|\overrightarrow{U_g} - \overrightarrow{U_l}\right|, \qquad (4)$$

where C_D is the drag coefficient and $A_{gl} = 6r_g/d_g$ is the interfacial area per unit of volume of an ensemble of particles of diameter d_g and volume fraction r_g. The expression for the drag coefficient varies according to the multiphase system. In this work, the drag force model used was the Ishii-Zuber model, which considers the bubble deformation:

$$C_D^{(dist)} = min\left(C_D(ellipse), C_D(cap)\right)$$
$$C_D = max\left(C_D(sphere), C_D(dist)\right) \quad (5)$$

$$C_D^{ellipse} = \frac{2}{3} E_O^{1/2} E(r_d) \quad (6)$$

$$E(r_d) = \frac{\left(1+17.67 f(r_d)^{6/7}\right)}{18.67 f(r_d)}, \quad f(r_d) = \frac{\mu_l}{\mu_m}(1-r_d)^{1/2}, \quad E_O = \frac{g\Delta\rho d_p^2}{\sigma} \quad (7)$$

where, E_O is the Etvos number, $\mu_m = \mu_l(1\text{-}r_g/r_{dm})^{-2.5 r g \mu^*}$ is the bulk viscosity and $\Delta\rho = \rho_l - \rho_g$.

$$C_D^{sphere} = \frac{24}{Re}(1 + 0.15\, Re_m^{0.687}), \quad Re_m = \frac{\rho_l \left|\overrightarrow{U_g} - \overrightarrow{U_l}\right|}{\mu_m} \quad (8)$$

$$C_D^{cap} = \frac{8}{3}(1-r_d)^2 \quad (9)$$

The turbulence model used was the standard k-epsilon, which was used only for the continuous phase. This model was chosen since it has been recognized to provide satisfactory results in bubble columns flow simulations [5]. The parameters values of $C_\mu = 0.09$, $C_{\varepsilon 1} = 1.44$, $C_{\varepsilon 2} = 1.92$, $\sigma_k = 1$ and $\sigma_\varepsilon = 1.3$ were used.

The MUSIG model was used for modeling the bubble size distribution. The population balance discretized equation in this model is written as:

$$\frac{\partial}{\partial t}\left(\rho_d r_d f_i\right) + \frac{\partial}{\partial x^i}\left(\rho_d r_d U_d^i f_i\right) = S_i \quad (10)$$

Defining the size fraction as $f_i = r_i / r_d$, r_i is the volume fraction of the i-group; r_d is the bubbles total volume fraction; x^i is the position component; and S_i is the source term, which contains the rates of bubble birth and death due to the breakup and coalescence:

$$S_i = B_{Bi} - D_{Bi} + B_{Ci} - D_{Ci} \quad (11)$$

The contributions to birth and death due to the breakup and coalescence processes are given respectively by

$$B_{Bi} = \rho_d r_d \left(\sum_{j>i} g(v_j; v_i) f_j \right); \quad D_{Bi} = \rho_d r_d \left(f_i \sum_{j<i} g(v_i; v_j) \right) \quad (12)$$

$$B_{Ci} = (\rho_d r_d)^2 \left(\frac{1}{2} \sum_{j \le i} \sum_{k \le 1} Q(v_j; v_k) X_{jki} f_j f_k \frac{m_j + m_k}{m_j m_k} \right); \quad D_{Ci} = (\rho_d r_d)^2 \left(\sum_j Q(v_j; v_k) f_i f_j \frac{1}{m_j} \right) \quad (13)$$

where $g(v_j; v_i)$ is the specific breakup rate, $Q(v_j; v_k)$ is the specific coalescence rate and X_{jki} is the fraction of mass due to coalescence between the jth and the kth groups which goes to group i.

$$X_{jki} = \begin{cases} \dfrac{(m_j + m_k) - m_{i-1}}{m_i - m_{i-1}} & if \quad m_{i-1} < m_j + m_k < m_i \\ \dfrac{m_{i+1} - (m_j + m_k)}{m_{i+1} - m_i} & if \quad m_i < m_j + m_k < m_{i+1} \end{cases} \tag{14}$$

In this work the Luo and Svendsen breakup model was used to describe the bubble breakup. The breakup rate is written as

$$g(v_i; f_B v_i) = 0.923 F_B (1 - r_d) \left(\frac{\varepsilon_C}{d_i^2}\right)^{1/3} \int_{\xi_{min}}^{1} \frac{(1+\xi)^2}{\xi^{11/3}} e^{-\chi} d\xi \tag{15}$$

$$\text{where } \chi = \frac{12\left[f_{BV}^{2/3} + (1 - f_{BV})^{2/3} - 1\right]\sigma}{\beta \rho_c \varepsilon_c^{2/3} d_i^{5/3} \xi^{11/3}} \tag{16}$$

Here, F_B is a calibration coefficient, β=2 and ξ is the dimensionless size of eddies in the inertial subrange of isotropic turbulence:

$$\xi_{min} = 11.4 \frac{\eta}{d_i}; \qquad \eta = \left(\frac{1}{\varepsilon_c} \nu_c^3\right)^{1/4} \tag{17}$$

ε_C is the continuous phase eddy dissipation rate, ν_c is the continuous phase kinematic viscosity and σ is the surface tension coefficient.

For the coalescence process, the Prince and Blanch model was used, which models the coalescence by a collision rate of two bubbles and a collision efficiency relating to the time required for coalescence:

$$Q(v_i; v_j) = (\theta_{ij}^T + \theta_{ij}^B + \theta_{ij}^S)\eta_{ij}; \quad \eta_{ij} = e^{-t_{ij}/\tau_{ij}} \tag{18}$$

$$t_{ij} = \left(\frac{\rho_c r_{ij}^3}{16\sigma}\right) ln\left(\frac{h_0}{h_f}\right); \qquad \tau_{ij} = \frac{r_{ij}^{2/3}}{\varepsilon_c^{1/3}}; \qquad r_{ij} = \left[\frac{1}{2}\left(\frac{1}{r_i} + \frac{1}{r_j}\right)\right]^{-1} \tag{19}$$

where η_{ij} is the collision efficiency; t_{ij} is the time required for coalescence; τ_{ij} is the actual contact time during the collision; h_0 is the initial film thickness and h_f is the critical film thickness when the bubble rupture occurs, which are chosen as 1.10^{-4} and 1.10^{-8}m respectively; and r_{ij} is the equivalent radius.

The expressions for the collision contributions due to θ_{ij}^T turbulence and θ_{ij}^B buoyancy are shown below; the share contribution θ_{ij}^S is neglected:

$$\theta_{ij}^T = F_{CT} S_{ij} (u_{ti}^2 + u_{ij}^2)^{1/2}; \quad \theta_{ij}^B = F_{CB} S_{ij} \left| U_{rj} - U_{ri} \right| \tag{20}$$

where: $S_{ij} = \frac{\pi}{4}(d_i + d_j)^2$ is the interfacial area, $u_{ti} = \sqrt{2}\varepsilon_c^{1/3} d_i^{1/3}$ is the turbulence velocity, F_{CT} and F_{CB} are calibration factors and $U_{ri} = [(2.14\sigma/\rho_c d_i) + 0.505 g d_i]^{1/2}$.

Simulation Set up

The geometry used in this work consisted in a cylindrical bubble reactor with an external loop, as shown in Figure 1. The mesh used contained approximately 55 thousand control volumes, which were chosen after performing mesh independence tests. The results were compared with the experimental data of Wang, [12], who presented data for a column height of 4.6m.

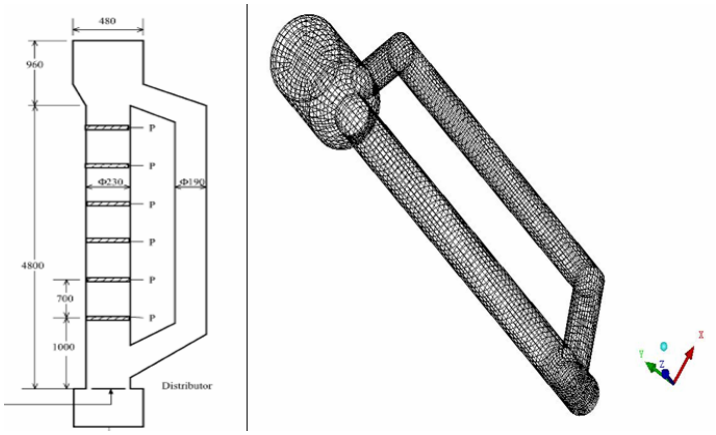

Figure 1: Bubble column reactor and mesh.

Simulations were performed considering air and water at 25ºC as dispersed and continuous phases, respectively. The column was assumed to be initially filled up to a height of 5 m. Non-slip conditions were adopted for both phases and for the time step, a step function was used from 0.00001 to 0.01s. A mean bubble size of 4mm was used. Two kinds of inlets were tested: one uniform and the other with a gas distributor with 133 holes, each 1mm in diameter; the former referred to a sintered plate entrance and the latter to a perforated plate entrance in the experimental system. Gas superficial velocities of 0.008, 0.016 and 0.032 m/s were simulated for both geometries. The tests referring to the breakup and coalescence phenomena were achieved only with the uniform inlet and the air superficial velocity of 0.032 m/s. For the test with the population balance models, air was assumed to be the polydispersed phase, with six bubble size groups varying according to a probability density function [12]. The bubble diameter is shown in Table 1.

Table 1: Bubble groups used in population balance simulations

Group	**1**	**2**	**3**	**4**	**5**	**6**
Diameter (mm)	0.5	1.5	2.4	3.3	4.2	7.0

For the initial condition, bubble group 2 was considered as 1 because of the correlation proposed by Chen, [3], in which the bubble diameter at the inlet is a function of the orifice diameter given by $d_b = 2.9(\sigma.d_o/\rho_l g)^{1/3}$; where d_b is the bubble diameter, σ is the surface tension coefficient, ρ_l is the liquid density and do is the orifice diameter, considered to be 30μm, which is the average pore size of the sintered plate used in the work of Wang, [12]. All simulations were performed in a commercial CFD package, CFX 11 from ANSYS; in all tests real-time simulation was approximately 200 seconds.

Results and Discussion

For the gas superficial velocity of 0.008 m/s (Figure 2), it is observed that the simulation results for the uniform gas entrance were in good agreement with experimental data; however, for the perforated plate case, simulations show an increase in the gas holdup near the wall, which is not corroborated by the experimental data.

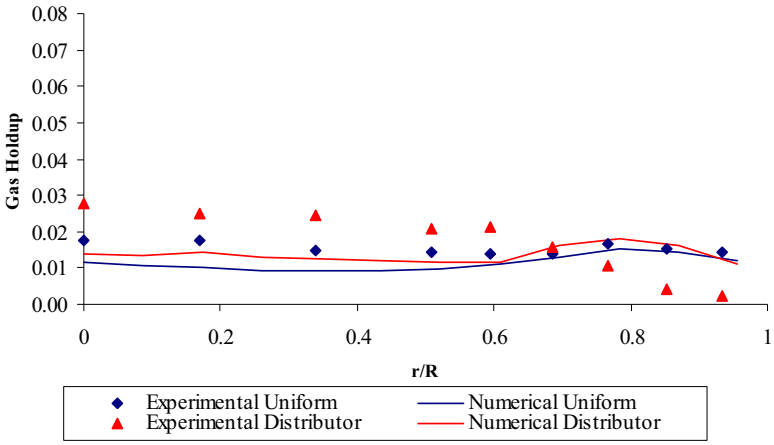

Figure 2: Gas holdup at 0.008 m/s

In Figure 3 it is shown the gas superficial velocity of 0.016 m/s. Here, different behaviors are observed for the two inlets; for the uniform inlet a uniform radial profile is noted, whereas for the perforated plate lower values of gas holdup near the wall are observed. For both gas entrances, simulations were in qualitative agreement with experimental data.

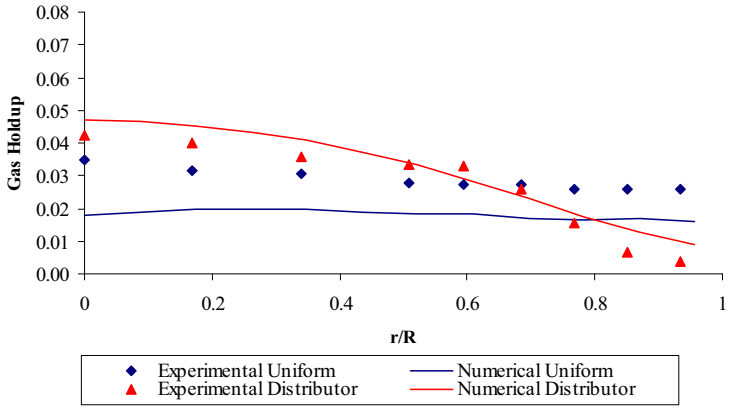

Figure 3: Gas holdup at 0.016 m/s

For the case in which the gas superficial velocity was 0.032 m/s showed in the Figure 4 is observed a decrease in gas holdup near the wall for both geometries. In this case, good agreement was obtained for the perforated plate distributor.

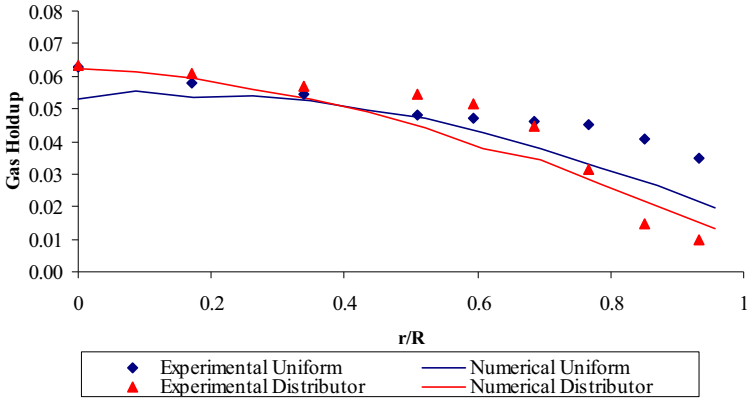

Figure 4: Gas holdup at 0.032 m/s

It was also evaluated the liquid axial velocities, where experimental data were not available. Liquid axial velocities were analyzed at three different heights in the column with the uniform and the perforated plate entrances at gas superficial velocities of 0.008; 0.016 and 0.032 m/s as shown in Figures 5, 6 and 7 respectively.

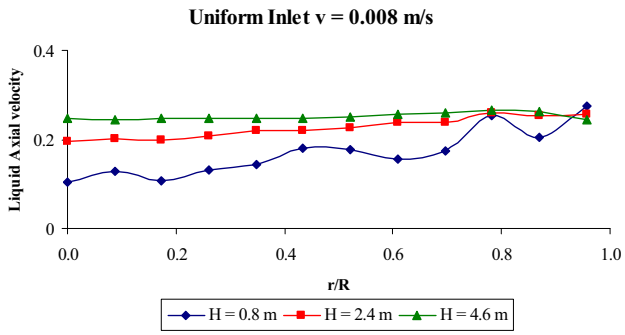

(a)

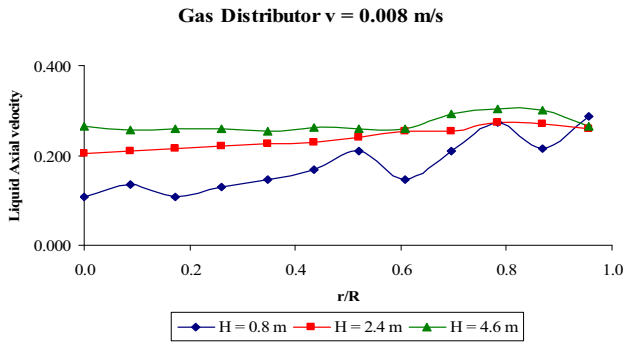

(b)

Figure 5: Liquid axial velocity at 0.008 m/s

At the gas superficial velocity of 0.008 m/s, the case with the gas distributor (Figure 5b) showed higher velocity values near the wall at the top of the column. For both cases higher velocity values near the wall were also observed at H=0.8m.

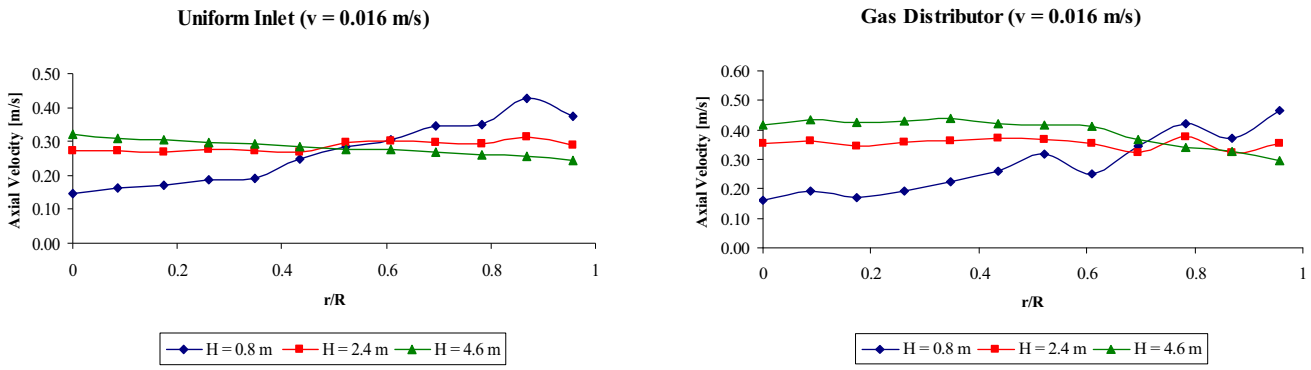

(a) (b)

Figure 6: Liquid axial velocity at 0.016 m/s

At the gas superficial velocity of 0.016 m/s (Figure 6), the obtained profile from the middle to the top of the column is almost constant, with the higher liquid axial velocity near the entrance of the gas.

For the case with the higher gas superficial velocity studied, shown in Figure 7, it also can be observed that only the profile at the bottom of column showed an increase from the center to the wall, as showed at the gas superficial velocity of 0.016 m/s.

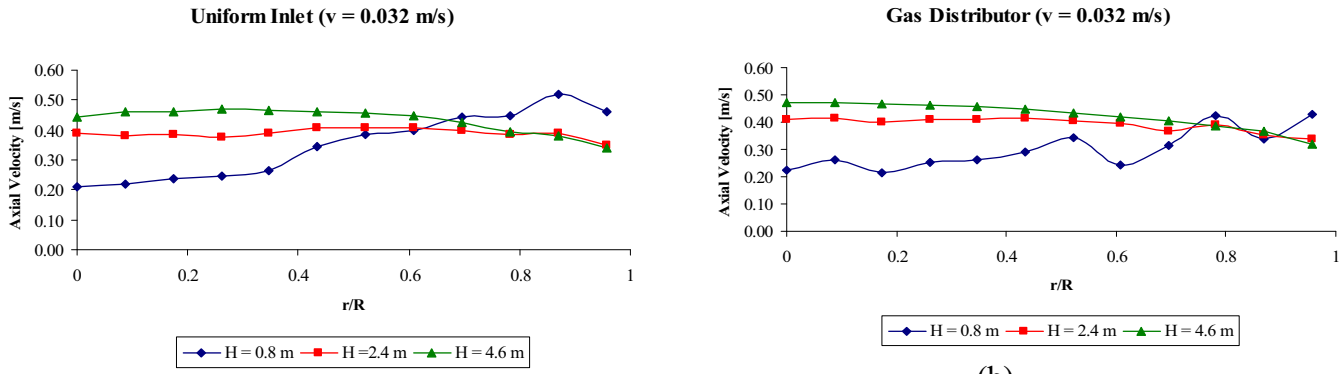

(a) (b)

Figure 7: Liquid axial velocity at 0.032 m/s

In all cases studied, liquid axial velocity profiles did not show dependence on the radial position for the uniform entrance and exhibited small variations for the perforated plate entrance only at the bottom of the column. The liquid axial velocity profiles were qualitatively similar, varying in magnitude due to the different values of the gas superficial velocity at the entrance.

Break up and coalescence models were evaluated at the gas superficial velocity of 0.032 m/s for the uniform entrance. It was considered six different bubble sizes and the size fraction of each diameter is shown in Figure 8.

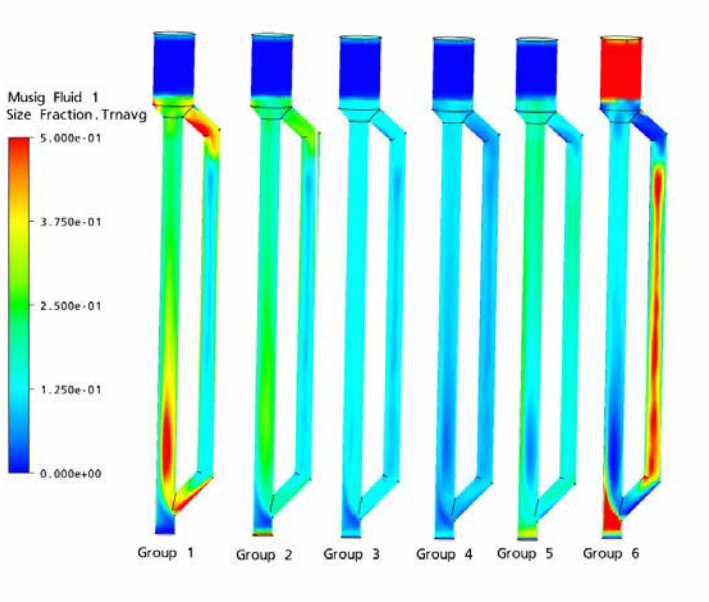

Figure 8: Bubble groups

It is noted that the bubbles of the group 1 are concentrated in the center of the column mostly at the bottom and in the recirculation zones of the external loop. The size fraction profiles of size groups 2 to 5 are similar; the bubbles are more concentrated at the center of the column and at the external loop. For group 6, bubbles appeared regularly at the center of the external loop, as well as at the top of the column, where initially there is only air, and at the bottom near the gas entrance.

The comparison between experimental data, simulation with a mean bubble diameter, and simulation with the bubble size distribution is presented in the Figure 9.

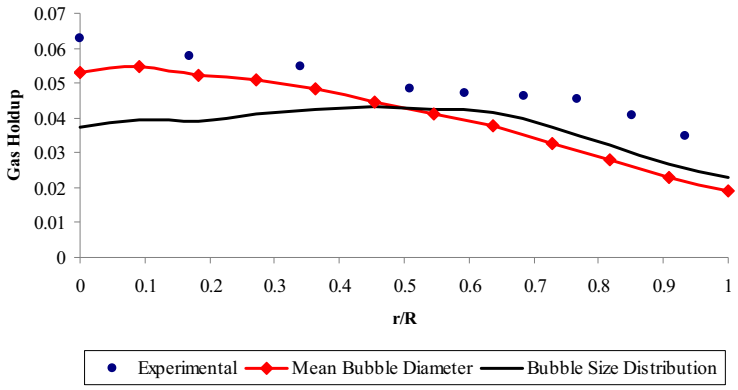

Figure 9: Gas holdup at the 4.6 m height

It is noted that the breakup and coalescence models underpredicted the average gas holdup in the region close to center of the column, whereas the gas holdup prediction is similar to that without the population balance models in the region close to the column wall. Although that homogeneous flow regime would be expected for an air/water system at the gas superficial velocity of 0.032 m/s, effects on the flow field due to the population balance modeling can be observed.

In Figure 10, gas holdup profiles for both regimes are shown. A higher concentration of air at the external loop is observed when the population balance was used. Further studies are currently being performed in the heterogeneous regime.

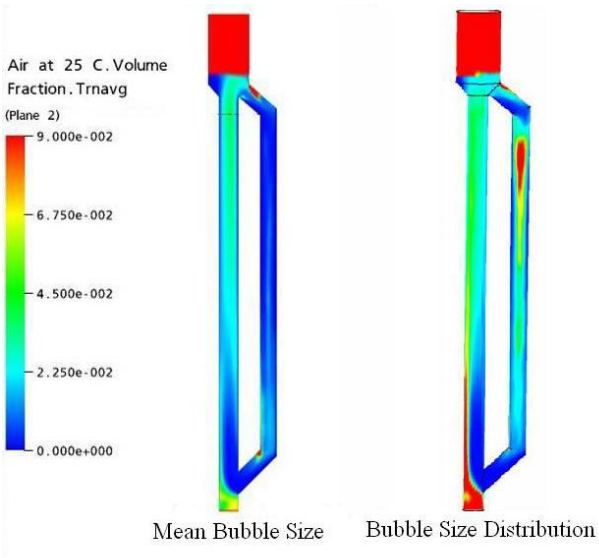

Figure 10: Gas holdup profiles

Liquid axial velocity profiles were compared only with the ones obtained with a mean bubble size, since experimental data is unavailable as mentioned before. Figures 11, 12 and 13 show the liquid axial velocity profiles at 0.8; 2.4 and 4.6 m of height respectively and 0.032 m/s of gas superficial velocity.

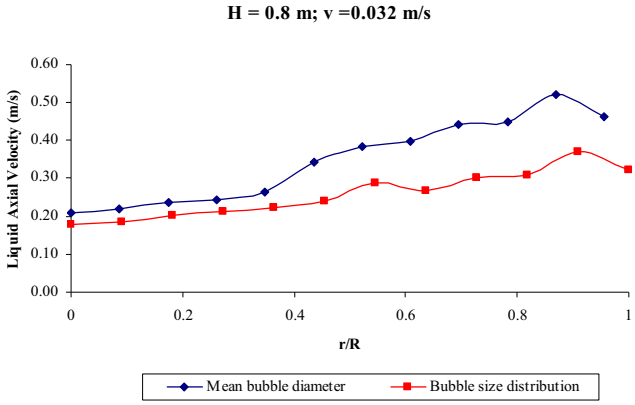

Figure 11: Liquid axial velocity at 0.8 m

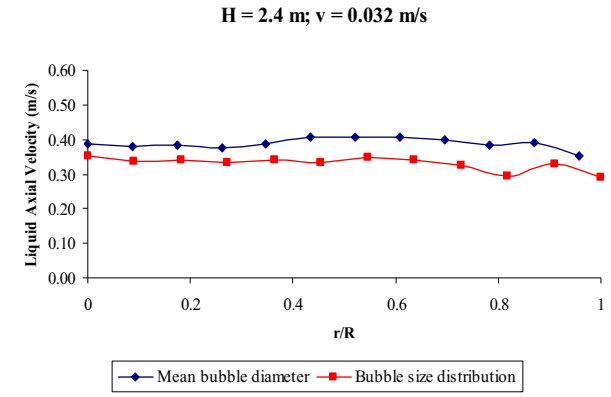

Figure 12: Liquid axial velocity at 2.4 m

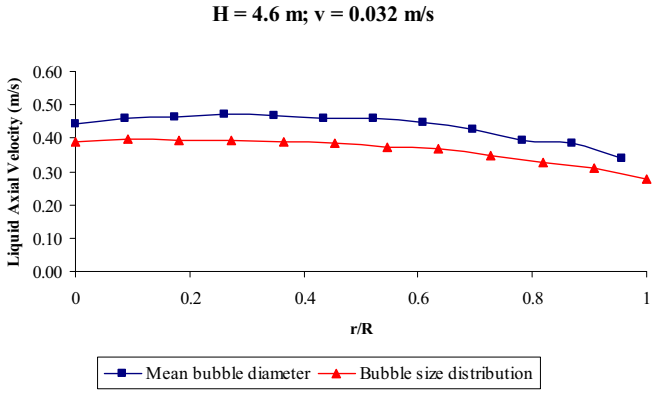

Figure 13: Liquid axial velocity at 4.6 m

It is observed that the data in which the break up and coalescence models are applied are in qualitatively agreement with the ones without consideration of the population balance. It is also noted that all profiles obtained with the break up and coalescence phenomena underpredicted the average liquid axial velocity along the radius of the column for all the heights measured.

Conclusion

This article presented gas-liquid flow CFD simulations in a cylindrical bubble reactor with an external loop, where the effects of different kinds of inlets and the influence of the implementation breakup and coalescence models were evaluated. The results of gas holdup corresponding to the different inlet types show good agreement with the experimental data. Axial velocity profiles obtained numerically did not show a considerable influence of the gas sparger. In evaluating the break up and coalescence models the results showed a decrease in the gas holdup at the center of the column, and the liquid axial velocity profiles were smaller along the column height when compared to simulations without break up and coalescence effects, showing the influence of the population balance implementation.

References

1. Akhtar, M. A., Tadé, M. O., Pareek, V. K. (2006), "Two-Fluid Eulerian Simulation of Bubble Column Reactors with Distributors", *J. Chem. Eng. Japan*, Vol. 39, pp. 831-841.

2. Cassanelo, M., Larachib, F., Kemoun, A., Al-Dahhan, M. H., Dudukovic, M. P. (2001), "Inferring Liquid Chaotic Dynamics in Bubble Columns Using CARPT", *Chemical Engineering Science*, Vol. 56, pp. 6125-6134.

3. Chen, P., Sanyal, J., Dudukovic, M. P. (2005), "Numerical Simulation of Bubble Columns Flows: Effect of Different Breakup and Coalescence Closures", *Chemical Engineering Science*, Vol. 60, pp. 1085-1101.

4. Krishna, R., Van Baten, J. M., Urseanu, M. I., Ellenberger, J. (2001), "A Scale up Strategy for Bubble Column Slurry Reactors", *Catalysis Today*, Vol. 66, pp. 199-207.

5. Krishna, R., Van Baten, J.M., Urseanu, M.I. (2004), "Three-phase Eulerian Simulations of Bubble Columns Reactors Operating in the Churn-turbulent Regime: A Scale up Strategy", *Chemical Engineering Science*, Vol. 55, pp. 4483-4493.

6. Luo, H., Svendsen, H.F. (1996), "Theoretical Model for Drop and Bubble Breakup in Turbulent Dipersions", *AIChE Journal*, Vol. 42, No. 5, pp. 1225-1233.

7. Maretto, C., Krishna, R. (1999), "Modelling of a Bubble Column Slurry Reactor for Fischer-Tropsch Synthesis", *Catalysis Today*, Vol. 52, pp. 279-289.

8. Matonis, D., Gidaspow, D., Bahary, M. (2002), "CFD Simulations of Flow and Turbulence in a Sulrry Bubble Column", *AIChE Journal*, Vol. 48, No. 7, pp. 1413-1429.

9. Prince, M.J., Blanch, H.W. (1990), "Bubble Coalescence and Break-up in Air-Sparged Bubble Columns", *AIChE Journal*, Vol. 36, No. 10, pp. 1485-1499.

10. Santos, C.M., Dionísio, R. P., Cerqueira, H.S., Sousa-Aguiar, E.F., Mori, M., d´Avila, M.A. (2007), "Three-Dimensional Gas-Liquid CFD Simulations in Cylindrical Bubble Columns", *The International Journal of Chemical Reactor Engineering*, Vol. 5, A90.

11. Van Baten, J. M., Ellenberger, J., Krishna, R. (2004), "CFD Modeling of a Bubble Column Reactor Carrying out a Consecutive A->B->C Reactoin", *Chem. Eng. and Tech.*, Vol. 27, No. 5, pp. 398-406.

12. Wang, T., Lin, J., Han, M., Zhang, T., Wang, J., Jin, W. (2004), "Influence of the Gas Distributor on the Local Hydrodynamic Behavior of an External Loop Airlift Reactor", *Chemical Engineering Journal*, Vol. 102, pp. 51-59.

13. Wiemann, D., Mewes, D. (2005), "Prediction of Backmixing and Mass Transfer in Bubble Columns Using a Multifluid Model", *Ind. Eng. Chem. Res.*, Vol. 44, pp. 4959-4967.